Published by Avanti Publishers

Global Journal of Earth Science and Engineering

ISSN (online): 2409-5710

Origin and Evolution of Geofluids in the Eocene Red-Bed Sandstones of the Dongying Depression, China: Constraints from Fluid Inclusions in Authigenic Minerals

Jian Wang[1,*], Mingfeng Xie[1], Alessandra Costanzo[2], Martin Feely[2], Yingchang Cao[1] and Keyu Liu[1,3]

[1]School of Geosciences, China University of Petroleum (East China), Qingdao 266580, China

[2]Earth and Ocean Sciences, School of Natural Sciences, National University of Ireland, Galway, Ireland

[3]Department of Applied Geology, Curtin University, GPO Box U1987, Perth, WA 6845, Australia

ARTICLE INFO

Article Type: Research Article

Keywords:
Eocene
Red-bed
Fluid inclusion
Diagenetic fluid
Sandstone reservoirs
Dongying depression

Timeline:
Received: November 10, 2021
Accepted: January 05, 2022
Published: March 11, 2022

Citation: Wang J, Xie M, Costanzo A, Feely M, Cao Y, Liu K. Origin and Evolution of Geofluids in the Eocene Red-Bed Sandstones of the Dongying Depression, China: Constraints from Fluid Inclusions in Authigenic Minerals. Glob J Earth Sci Eng. 2022; 9: 16-33.

DOI: https://doi.org/10.15377/2409-5710.2022.09.2

*Corresponding Author
Email: wangjian8601@upc.edu.cn
Tel: +86 18366201873

ABSTRACT

Fluid inclusion and petrographic study focused on authigenic quartz, annealed microfractures in quartz grains (AMF) and carbonate cement, was performed in red-bed reservoir sandstones from the first member of the Kongdian Formation and the lower fourth member of the Shahejie Formation (Shengli oilfield, East China). Both hydrocarbon and aqueous inclusions are present. Microthermometry and Laser Raman spectroscopes of liquid-rich two-phase inclusions showed that the pressure-correction value of aqueous inclusions is < 15°C. Differences in homogenization temperature and salinity occur between inclusions in quartz and carbonate cements. The liquid-rich two-phase aqueous inclusions were classified into four groups based on the salinity-homogenization temperature plots. The liquid-rich two-phase hydrocarbon inclusions were classified into two groups. The timing of the first-stage diagenetic fluid was before 31.3Ma. Fluids were from syn-depositional water and diagenetic fluids of clay minerals in interbedded mudstones. The timing of the second-stage diagenetic fluid was between 31.3 and 26.4Ma. Fluids were rich in organic acids and were accompanied by filling of small amounts of low maturity oil. The timing of the third-stage diagenetic fluid was between 26.4 and 21.4Ma. Fluids were mainly influenced by dehydration of gypsum-salt rocks and decarboxylation of organic acids. The timing of the fourth-stage diagenetic fluid was after 21.4 Ma. Fluids were influenced by organic acids and carbon acids and were accompanied by filling of mature oil after 10Ma. During the burial history, the red-bed reservoirs experienced the evolution process of early alkaline diagenetic fluids, early acid diagenetic fluids, late alkaline diagenetic fluids and late acid diagenetic fluids, which caused the alternate evolution of multiple alkaline and acid diagenetic environments.

1. Introduction

The diagenesis of sedimentary rocks in a sedimentary basin is the interactional process between water and rocks [1,2]. Formation fluids represent a key factor in the evolution of the diagenetic environment and act as reaction media in the process of diagenesis [1,3]. The evolution of fluids in a sedimentary basin is influenced by thermal evolution of organic materials [4,5], clay minerals [6,7] and gypsum-salt deposits [8] and other sources [9] on the basis of primary sedimentary water [10,11]. Properties of reservoir fluids varied frequently during the burial history, causing different diagenetic environments and multiple diageneses in clastic reservoirs in one area at different stages [12]. Diagenetic authigenic minerals in clastic reservoirs mainly occur as authigenic quartz, carbonate cements (calcite, ferro-calcite and ankerite), sulfate cements (gypsum and anhydrite), siderite and authigenic clay minerals. Crystallization of the diagenetic minerals in reservoir rocks begins during sedimentation and continues through the burial and uplift history of the sedimentary basin. During the crystallization of diagenetic minerals, fluids, such as water, oil and gas are trapped within the crystals as inclusions. This records the information on formation fluids in the evolving sedimentary basin [13-17]. Authigenic quartz usually forms in acidic diagenetic environments, while carbonate cement and sulfate cement form in alkaline diagenetic environments [18,19]. Fluid inclusions hosted in authigenic quartz, carbonate cements and annealed fractures record different types of fluids and provide the most direct evidence for the evolution of the diagenetic fluids, which is the basis for studying the diagenesis of reservoirs.

Preliminary studies show that the diagenesis of red-bed reservoirs was reflected by the formation of multiple diagenetic cements, *e.g*., authigenic quartz, calcite, ferrocalcite, ankerite, gypsum and anhydrite [20]. We present the results of an extensive liquid-rich two-phase fluid inclusion study mainly focusing on authigenic quartz cements, carbonate cements and AMF in red-bed reservoir sandstones from the Shengli oilfield in East China. Temperature and salinity measurements were obtained and pressure-correction of homogenization temperature of each individual inclusion has been estimated based on the Laser Raman spectroscopy study. The evolution history of the diagenetic fluids in red-bed reservoirs in the Dongying Depression was reconstructed based on the study of fluid inclusions.

2. Geological Background

The Bohai Bay Basin is an important hydrocarbon producing basin. It is located on the eastern coast of China and covers an area of approximately 200,000 km^2. It is a rifted basin formed in the Late Jurassic through to the early Tertiary on the basement of the North China platform. The tectonic evolution of the basin consists of a syn-rift stage (65.0-24.6 Ma) and a post-rift stage (24.6 Ma to the present). The post-rift stage occurred during the deposition period of the Guantao, Minghuazhen, and Pingyuan Formations.

The Bohai Bay Basin consists of several subbasins (Fig. **1A**). The Dongying Depression is a secondary tectonic unit of the Jiyang Subbasin and covers an area of 5700 km^2. The Qingtuozi Bulge occurs in the east, the Guangrao Bulge in the southeast, the Luxi Uplift in the south, the Gaoqing Bulge in the west and the Chenguangzhuang Bulge in the north (Fig. **1B**). According to tectonic characteristics, the Dongying Depression can be subdivided into five tectonic belts from north to south. They are the Northern Steep Slope Belt, the Northern Sag (Lijin sag and Minfeng sag) Belt, the Central Fault Anticline Belt, the Southern Sag (Boxing sag and Niuzhang sag) Belt, and the Southern Gentle Slope Belt. The study area includes the Boxing sag, the Niuzhuang sag and the Southern Gentle Slope Belt.

The depression was filled with Cenozoic sediments, which were composed of the Paleogene Kongdian (*Ek*), Shahejie (*Es*) and Dongying (*Ed*) formations, the Neogene Guantao (*Ng*) and Minghuazhen (*Nm*) formations and the Quarternary Pingyuan (*Qp*) Formation (Fig. **2A**). Influenced by the Himalayan movement, the syn-rift basin experienced three stages: initial rift stage (*Ek* and the fourth member of *Es* (*Es4*)), strong rift stage (the third member of *Es* (*Es3*) and lower second member of *Es* (*Es2x*)) and atrophic rift stage (the upper second member of *Es* (*Es2s*), the first member of *Es* (*Es1*) and *Ed*) [21], which comprised the sedimentary cycle with the sequence of shore-shallow lacustrine facies-deep lacustrine facies-fluvial and shore-shallow lacustrine facies [22]. At the 24.6Ma the formations of *Ek* and *Es4* experienced tectonic uplift and re-subsidence events (Fig. **2B**). The average

paleo-geothermal gradient of the formations of *Ek* and *Es4* was > 53.5°C/km, and the paleo-temperatures were modeled [23].

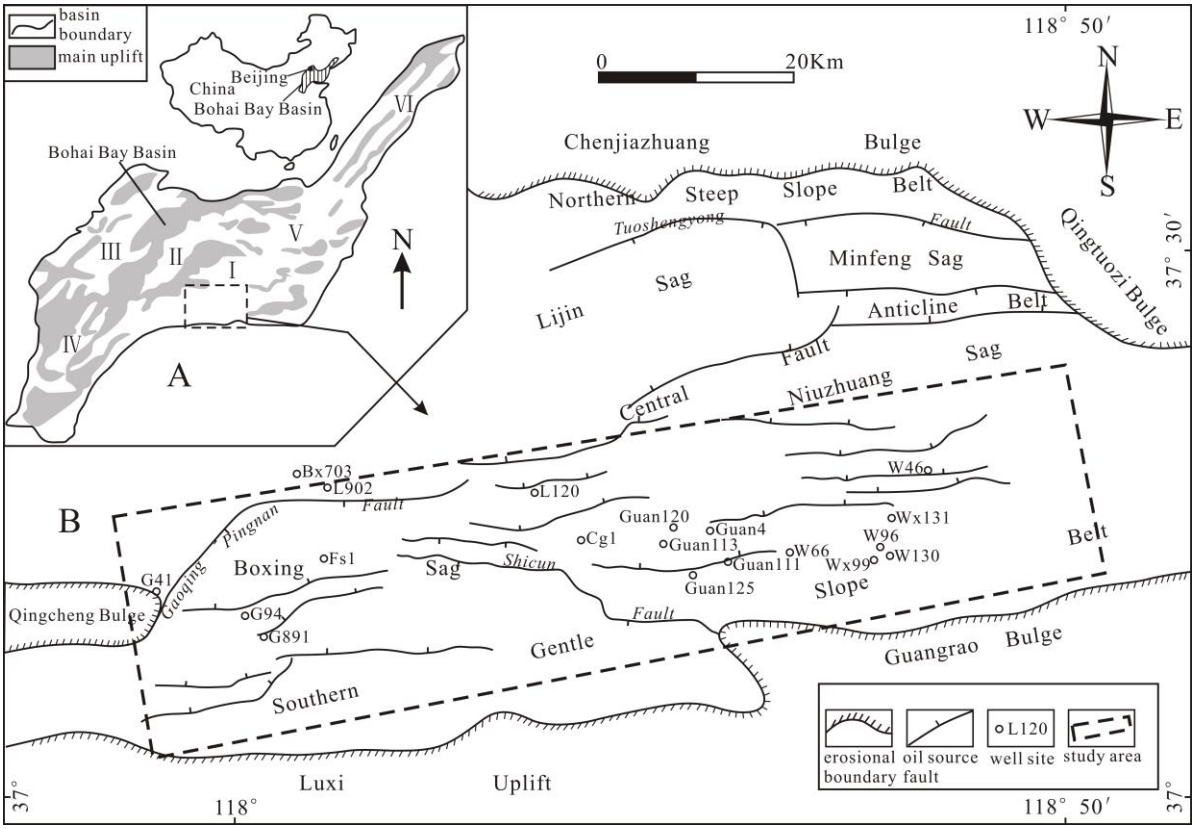

Figure 1: (A) Tectonic setting of the Dongying Depression in the southern Jiyang Subbasin (I) of Bohai Bay Basin. Other subbasins in the Bohai Bay Basin of North China are the Huanghua Subbasin (II), the Jizhong Subbasin (III), the Linqing Subbasin (IV), the Bozhong Subbasin (V) and the Liaohe Subbasin (VI). (B) Structural map of the Dongying depression with well locations and oil source faults of *Ek1-Es4x*.

3. Methodology

Twenty-four samples of red-bed sandstones of *Ek1-Es4x* from seventeen wells of the Dongying Depression were studied to record the type, abundance, distribution and size of fluid inclusions. Eight of these samples were prepared as doubly polished fluid inclusion wafers and subjected to fluid inclusion microthermometry at the Geofluids Research Laboratory, Earth and Ocean Sciences, National University of Ireland Galway. Fluid inclusion petrography and ultraviolet light microscopy were carried out at room temperature using a Nikon Eclipse E200 microscope equipped with an epifluorescence attachment. Microthermometry was carried out using a Linkam THMGS-600 heating freezing stage. Calibration of the stage was performed following the method outlined [24], in addition, synthetic fluid inclusion standards were used (pure CO_2 and water). Precision is ± 0.2°C at -56.5°C and ± 2°C at 300°C. The eutectic temperatures (T_e), last ice melting temperatures (T_{mice}) and homogenization temperatures (T_h) were observed at a heating rate of no more than 5°C/min.

The method of calculating pH of fluid inclusions is after Liu [25]. The formula applies to simple NaCl-H_2O aqueous inclusions, which was established on the basis of the thermodynamic property of ion reactions in aqueous inclusions, and combined with the formulas deduced [26,27]. Using the equilibrium constants of chemical reactions under higher pressure (>1bar), the problem of calculating pH parameters for the aqueous inclusions trapped under different conditions, especially at higher temperatures and pressures, is solved. The formula for calculating the pH of simple NaCl-H_2O aqueous inclusions at trapping conditions is as follows,

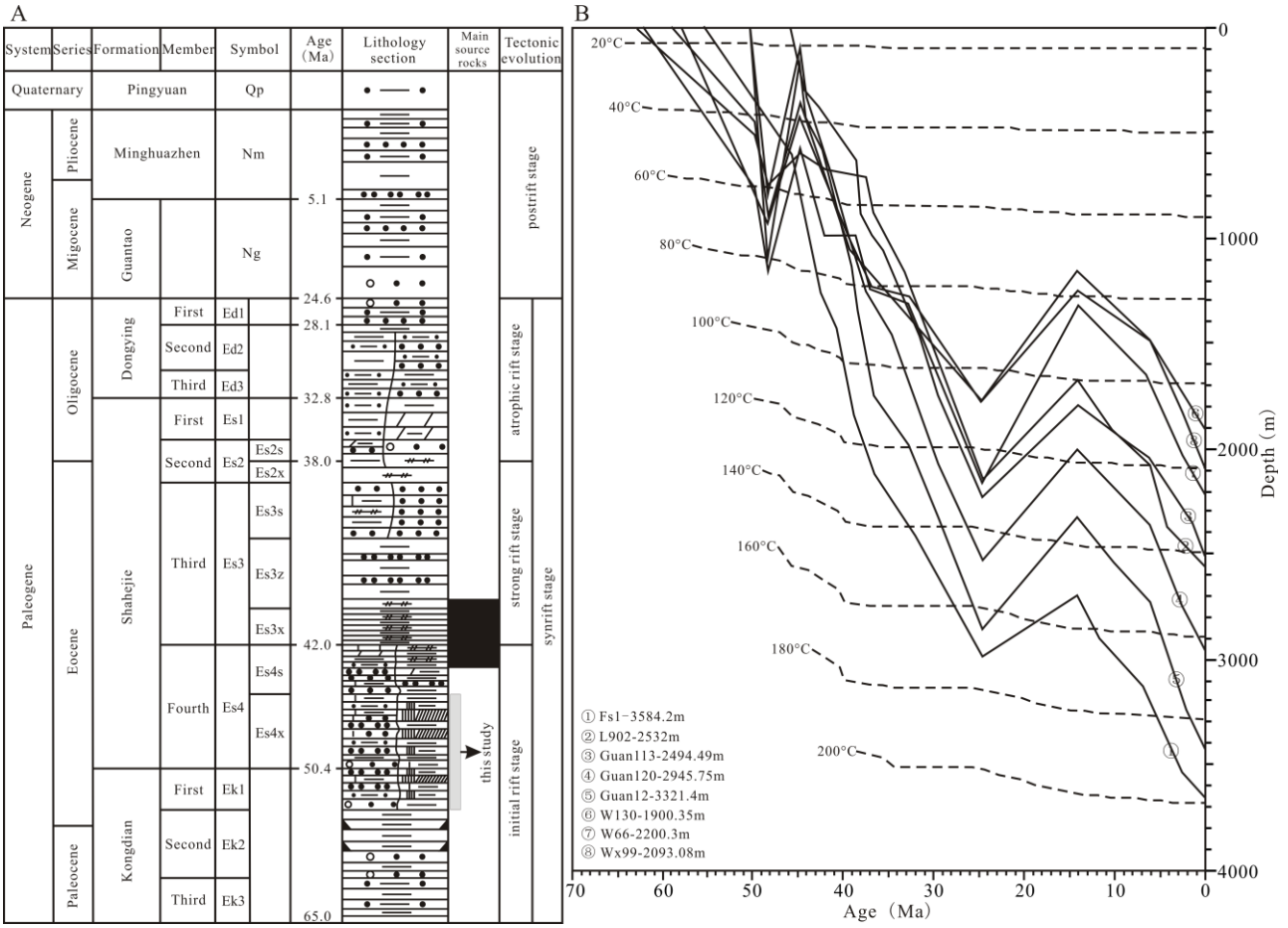

Figure 2: (A) Schematic Tertiary stratigraphy and tectonic evolution of the Dongying Depression. (B) Burial histories for the eight sample wells of the Dongying Depression. Temperatures were modeled [23]. See Figure **1B** for well locations. *QP*-Quaternary Pingyuan Formation; *Nm*-Neocene Minghuazhen Formation; *Ng*-Neocene Guantao Formation; *Ed1*-The first member of Paleogene Dongying Formation (*Ed*); *Ed2*-The second member of *Ed*; *Ed3*-The third member of *Ed*; *Es1*-The first member of Paleogene Shahejie Formation (*Es*); *Es2s*-The upper second member of *Es*; *Es2x*-The lower second member of *Es*; *Es3s*-The upper third member of *Es*; *Es3z*-The middle third member of *Es*; *Es3x*-The lower third member of *Es*; *Es4s*-The upper fourth member of *Es*; *Es4x*-The lower fourth member of *Es*; *Ek1*-The first member of Paleogene Kongdian Formation (*Ek*); *Ek2*-The second member of *Ek*; *Ek3*-The third member of *Ek*.

$$pH=-\log [H^+],\ [H^+]^2=K_w/(1+(m_{NaCl}*K_{NaCl})^{0.5}/K_{HCl}) \quad (1)$$

m_{NaCl}—Molar concentration of salinity of NaCl-H_2O aqueous inclusions

K_w, K_{NaCl} and K_{HCl}—Equilibrium constants (after [27])

4. Results

4.1. Fluid Inclusions Petrography

Fluid inclusions occur in authigenic quartz, detrital quartz grains, carbonate cement and AMF. Fluid inclusions in the first three kinds of host minerals are mainly primary, secondary in fractures. Fluid inclusions in quartz grains are inherited and trapped before the formation of the sedimentary rocks therefore do not record information of diagenetic fluids [28]. Fluid inclusions hosted in authigenic quartz, carbonate cement and AMF (Fig. **3**) are formed during the diagenetic stage of sedimentary rocks and record significant information on the diagenetic fluids [14, 29].

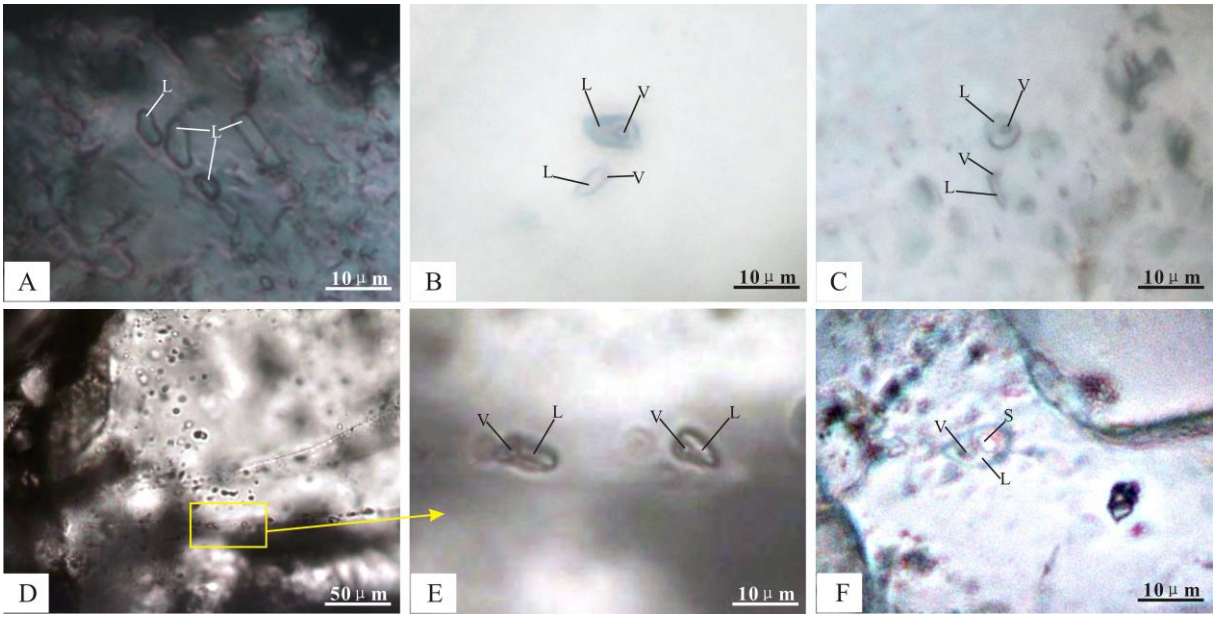

Figure 3: Aqueous inclusions in diagenetic authigenic minerals and AMF from red-bed sandstones of the Dongying Depression. (A) Primary ellipsoidal and negative crystal shape monophase inclusions in calcite, from well Wx99 at 1940.23m; (B) Primary ellipsoidal liquid-rich two-phase inclusions with F=0.92 in authigenic quartz, from well L902 at 2532.45m; (C) Primary oblate and tubular liquid-rich two-phase inclusions with F=0.95 in carbonate cement, from well Guan 113 at 2494.49m; (D) AMF and secondary ellipsoidal liquid-rich two-phase inclusions with F=0.93 in them, from well Fs1 at 3584.2m; (E) Enlargement of E; (F) Primary negative crystal shape multiphase solid inclusion with halite crystal in carbonate cement, from well W130 at 1900.35m.

Primary inclusions hosted in authigenic quartz and carbonate cements are usually isolated, occur in a three-dimensional random distribution and are parallel to growth zones of quartz or crystal faces of calcite. Secondary inclusions occur as trails along with the AMF. Five fluid inclusion morphologies were observed: oblate, ellipsoidal, tubular, triangular and negative crystal shape. Fluid inclusions sizes are small being usually less than 10μm with the majority ranging between 2 and 8μm in length. Fluid inclusions are classified into aqueous inclusions (Fig. **3**) and hydrocarbon inclusions (Fig. **4**). Aqueous inclusions are classified according to phases observed at room temperature into monophase (Ia), liquid-rich two-phase (Ib) and multiphase solid inclusion (Ic). Hydrocarbon inclusions mainly occur in AMF along with aqueous inclusions are classified into monophase (IIa) and liquid-rich two-phase (IIb) inclusions according to the phases observed at room temperature. Fluid inclusions are dominated by type Ib and IIb. The relationship between type I and type II inclusions are shown in Fig. (**5**). Type Ia and type Ic inclusions are mainly hosted in calcite as primary inclusions. Type Ib inclusions hosted in authigenic quartz, calcite and ferro-calcite are primary. Type Ib and Type II inclusions occurring as trails along the AMF are secondary. Primary inclusions hosted in authigenic quartz and carbonate cements are usually isolated, occur in a three-dimensional random distribution and are parallel to growth zones of quartz or crystal faces of calcite. The petrographic features of these inclusions are listed in Table **1**.

4.2. Fluid Inclusion Microthermometry

The microthermometric study was aimed at type Ib and IIb inclusions due to their predominance. The T_e of some large inclusions and the T_{mice} and T_h of most inclusions were recorded. The T_{mice} of some type I-b inclusions are >0°C and others in the same group are < 0°C.

The T_e of type Ib inclusions in authigenic quartz and AMF ranges between -29 and -20°C, which indicates that the fluid composition is mainly NaCl-H_2O. The T_{mice} of type Ib inclusions in carbonate cements ranges between -50 and -46°C, which indicates that the fluid composition is $CaCl_2$-H_2O. All of the type Ib and IIb inclusions are homogenized to liquid. When the salinity is <30wt %, the temperature-solubility relation of $CaCl_2$-H_2O system is similar to NaCl-H_2O system [30,31]. Hence, the salinities of all type Ib inclusions are given in weight percent NaCl equivalent on a NaCl-H_2O basis.

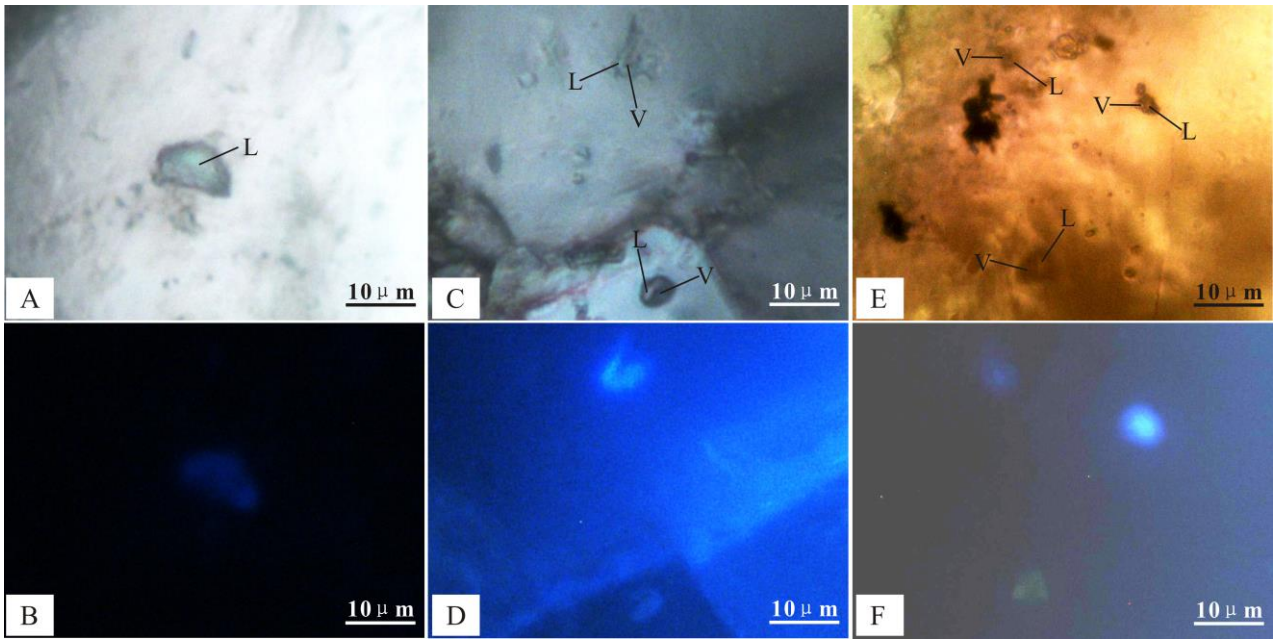

Figure 4: Hydrocarbon inclusions in diagenetic authigenic minerals in red-bed sandstones of the Dongying Depression. (A) Secondary inclusion in AMF with light green under normal light and (B) blue fluorescence under UV from well Fs1 at 3584.2m. (C) Secondary liquid-rich two-phase inclusions in AMF with light green under normal light and (D) yellow-green and blue fluorescence under UV from well Wx99 at 2093.04m. (E) Secondary liquid-rich two-phase inclusions in AMF with brown normal light and (F) blue, blue white and yellow fluorescence under UV from well L902 at 2532m.

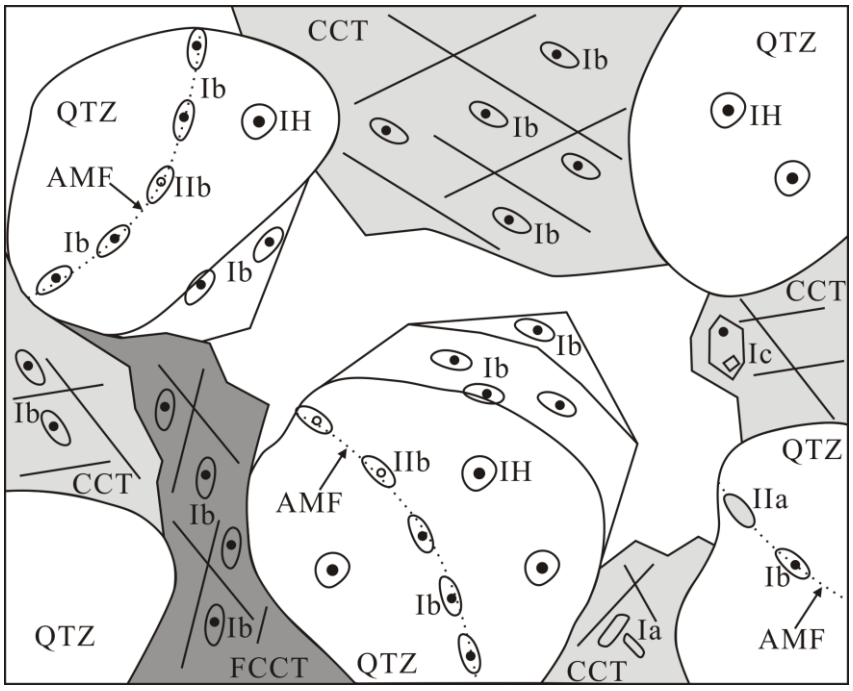

Figure 5: The relationship between type I and type II inclusions in red-bed sandstones of the Dongying Depression. Abbreviations: IH-inherited inclusion; QTZ-quartz; CCT-carbonate cement; FCCT-ferro-carbonate cement; AMF-annealed microfractures in quartz grain.

Sample 1 (Fs1-3584.2m): Primary inclusions in authigenic quartz have T_{mice} ranging between -8 and -0°C, corresponding to the salinities ranging between 1 and 11 eq.wt%NaCl; the T_h ranges from 100 to 170°C. Secondary inclusions in AMF have T_{mice} ranging between -8 and -0°C, corresponding to the salinities ranging between 1 and

Table 1: Summary of petrographic features of fluid inclusions in diagenetic minerals and AMF from red-bed sandstones of the Dongying Depression.

Features	Aqueous Inclusions			Hydrocarbon Inclusions	
	Ia	Ib	Ic	Iia	IIb
Host mineral	CCT	AQ, AMF and CCT	CCT	AMF	AMF
Genetic type	P	P and S	P	S	S
Color	colorless and transparent	colorless and transparent	colorless and transparent	light green or colorless under normal light; blue fluorescence under UV	light green, brown, light yellow or black under normal light; blue, yellow-green, yellow or blue white fluorescence under UV
Morphology	ellipsoidal and tubular	dominated by oblate, ellipsoidal and tubular	negative crystal shape	ellipsoidal	ellipsoidal
Length	2-6μm	2-8μm	4-9μm; daughter minerals<2μm	<8μm	3-8μm
Degree of fill	——	usually >0.85	——	——	usually >0.8
Abundance	low	high	very low	Low	relatively high

Abbreviations: AQ-authigenic quartz; P-primary inclusion; S-secondary inclusion; others as in Fig. (**5**).

11 eq.wt%NaCl; the T_h ranges from 120 to 160°C. Primary inclusions in carbonate cements have T_{mice} mainly ranging between -17 and -3°C, corresponding to the salinities ranging between 4 and 20 eq.wt%NaCl; the T_h is in the range of 120 to 180°C (Figs. **6A**, **7A**, **8A**).

Sample 2 (L902-2532m): The T_{mice} of primary inclusions in authigenic quartz ranges from -5 to 0°C, corresponding to the salinities ranging from 1 to 8 eq.wt%NaCl; the T_h ranges between 90 and 140°C. The T_{mice} of secondary inclusions in AMF is ranging between -9 and 0°C, corresponding to the salinities ranging from 1 to 15 eq.wt%NaCl (Figs. **6B**, **7B**, **8B**). Only three type Ib inclusions were observed in carbonate cements, the average T_{mice} is -9.1°C, and the average salinity is about 14 eq.wt%NaCl; the average T_h is about 93°C. The T_h of type IIb inclusions is in Table **2**.

Sample 3 (Guan113-2494.49m): The T_{mice} of primary inclusions in authigenic quartz ranges from -8 to -2°C, corresponding to the salinities ranging between 3 and 11 eq.wt%NaCl; the T_h is in the range of 80 to 150°C. The T_{mice} of secondary inclusions in AMF ranges from -12 to 0°C, and the salinities are from 1 to 16 eq.wt%NaCl; the T_h are between 80 and 130°C. The T_{mice} of primary inclusions in carbonate cements ranges from -21 to -7°C, and the salinities are from 11 to 23 eq.wt%NaCl; the T_h is in the range of 60 to 140°C (Figs. **6C**, **7C**, **8C**). The T_h of type IIb inclusions is in Table **2**.

Sample 4 (Guan120-2945.75m): The T_{mice} of primary inclusions in authigenic quartz ranges from -8 to -1°C, and the salinities are from 2 to 11 eq.wt%NaCl; the T_h ranges from 100 to 160°C. The T_{mice} of secondary inclusions in AMF ranges from -5 to -1°C, corresponding to the salinities ranging from 2 to 8 eq.wt%NaCl; the T_h is in the range of 100 to 130°C. The T_{mice} of primary inclusions in carbonate cements ranges from -21 to -1°C, and the salinities are between 3 and 23 eq.wt%NaCl; the T_h is in the range of 90 to 150°C (Figs. **6D**, **7D**, **8D**).

Sample 5 (Guan12-3321.4m): The T_{mice} of primary inclusions in authigenic quartz ranges from -6 to -1°C, and the salinities are between 3 and 9 eq.wt%NaCl; the T_h is in the range of 110 to 150°C. The T_{mice} of secondary inclusions in AMF ranges between -11 and -1°C, corresponding to the salinities ranging between 3 and 15 eq.wt%NaCl; the T_h is in the range of 110 to 150°C. The T_{mice} of primary inclusions in carbonate cements ranges from -21 to -10°C, and the salinities are from 14 to 23 eq.wt%NaCl; the T_h is in the range of 80 to 160°C (Figs. **6E**, **7E**, **8E**).

Sample 6 (W130-1900.35m): The T_{mice} of secondary inclusions in AMF ranges from -16 to -1°C, and the salinities are from 2 to 19 eq.wt%NaCl; the T_h ranges in the range of 80 to 130°C. The T_{mice} of primary inclusions in

carbonate cements ranges from -21 to -5°C, and the salinities are between 6 and 23 eq.wt%NaCl; the T_h is in the range of 80 to 130°C (Fig. **6F**, **7F**, **8F**).

Sample 7 (W66-2200.3m): The T_{mice} of primary inclusions in authigenic quartz ranges from -5 to -1°C, corresponding to the salinities ranging from 2 to 8 eq.wt%NaCl; the T_h is in the range of 70 to 120°C. The T_{mice} of secondary inclusions in AMF ranges from -17 to -1°C, and the salinities are from 2 to 20 eq.wt%NaCl; the T_h is in the range of 70 to 120°C. The T_{mice} of primary inclusions in carbonate cements ranges between -18 to -5°C, and the salinities are between 9 and 21 eq.wt%NaCl; the T_h is in the range of 60 to 120°C (Figs. **6G**, **7G**, **8G**).

Sample 8 (Wx99-2093.08m): The T_{mice} of secondary inclusions in AMF range from -10 to -1°C, corresponding to the salinities ranging between 2 and 14 eq.wt%NaCl; the T_h is in the range of 50 to 120°C (Fig.6H, 7H, 8H). The T_h of type IIb inclusions is in Table **2**.

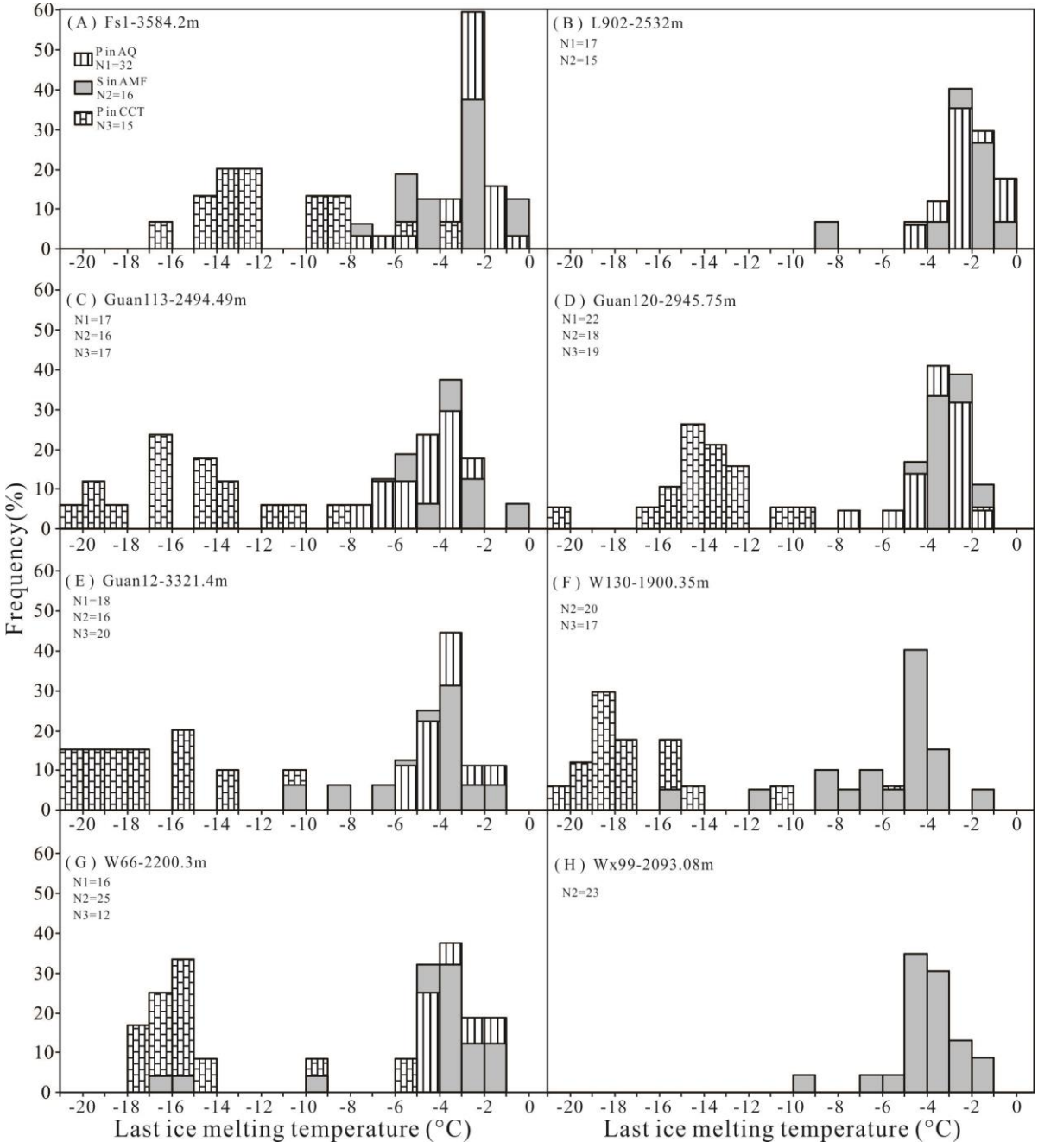

Figure 6: Histograms showing last ice melting temperatures for type Ib inclusions in the eight samples. Abbreviations as in Fig. (**5**) and Table **1**.

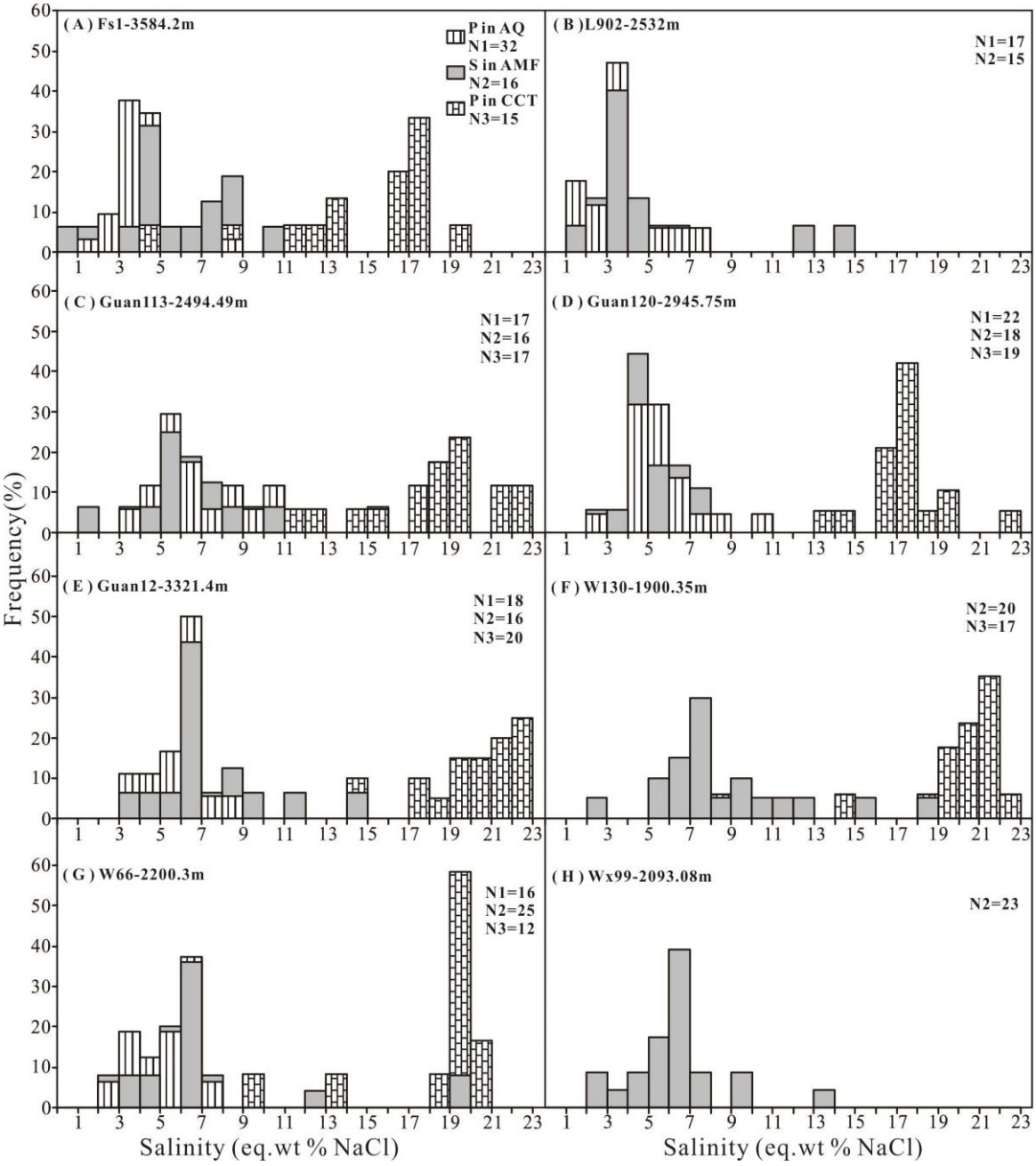

Figure 7: Histograms showing salinities for type Ib inclusions in the eight samples. Salinities are given in weight percent NaCl equivalent on a NaCl-H2O basis. Abbreviations as in Fig. (**5**) and Table **1**.

The T_h and salinities of secondary inclusions in AMF are similar to those of the primary inclusions in authigenic quartz, indicating that secondary inclusions in AMF may also be chemically related to the diagenetic fluids. The T_h of inclusions in carbonate cements are classified into two groups (Fig. **7A,B**). The T_h of inclusions in authigenic quartz and AMF mainly define one group with relatively low temperatures. Some samples have a high-temperature group in authigenic quartz and AMF (Fig. **7C**). Salinities of inclusions in carbonate cements are higher than that of inclusions in authigenic quartz and AMF. The T_h of hydrocarbon inclusions is 20-30°C lower than that of synchronous secondary aqueous inclusions (Table **2**).

4.3. Laser Raman Spectroscopy of Fluid Inclusions

Laser Raman Spectroscopy focused on type Ib inclusions, and the results show that the Raman Shifts of most inclusions have the high-intensity peaks in the range of 2887 cm^{-1} to 2930cm^{-1} and the range of 3080 cm^{-1} to

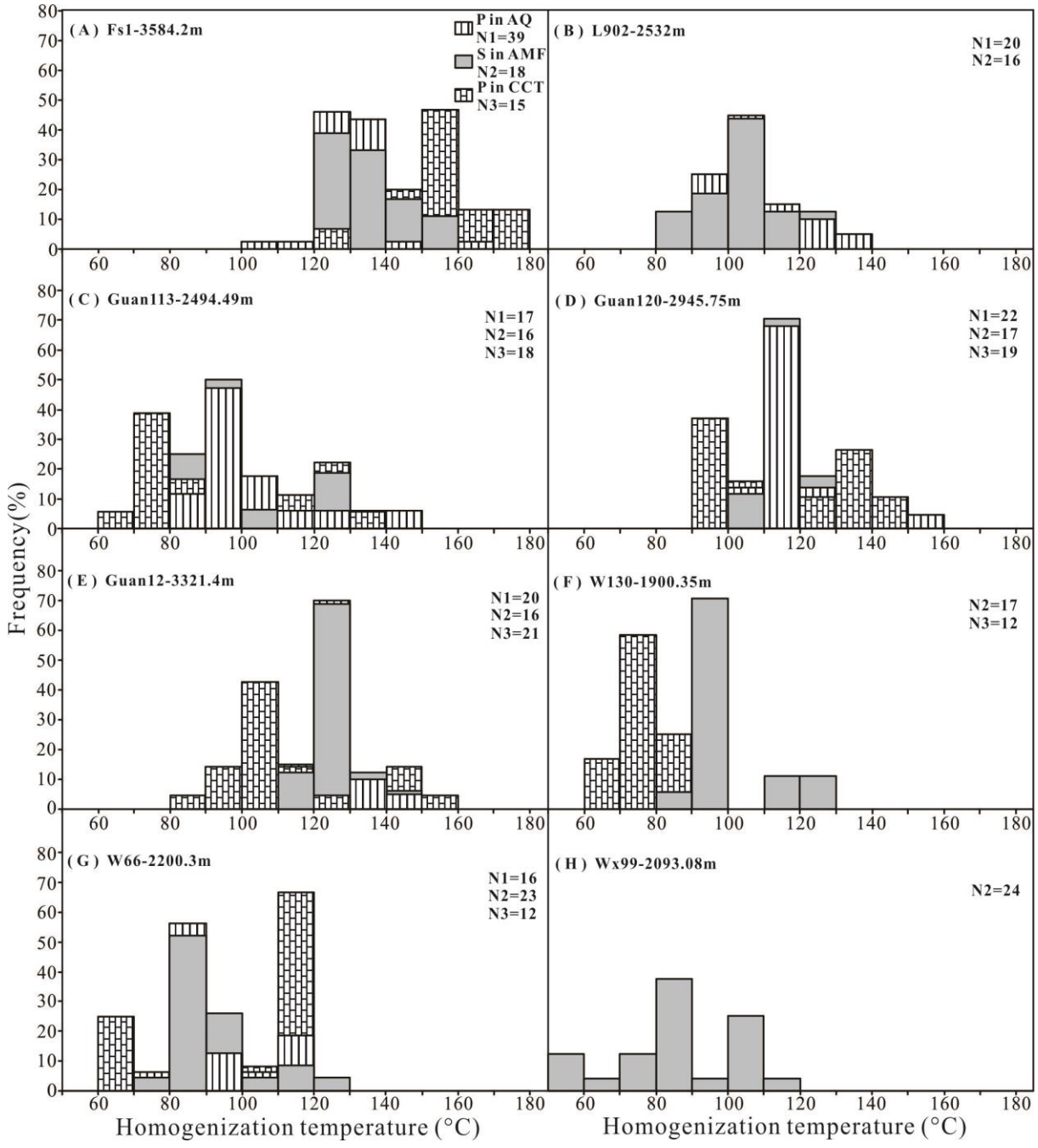

Figure 8: Histograms showing homogenization temperatures for type I-b inclusions in the eight samples. All of the inclusions homogenize to liquid. Abbreviations as in Fig. (**5**) and Table **1**.

3725cm^{-1} respectively (Fig. **9**), the former reflects the presence of methane (CH_4) and other short-chain hydrocarbons and the later reflects the presence of water (H_2O). Compared with the peak areas of H_2O, the peak areas of CH_4 are very small, which indicates that the content of CH_4 is very low [32].

5. Discussion

5.1. Trapping Temperature and Pressure

The T_h is the minimum fluid trapping temperature, and true trapping temperature cannot be obtained without a pressure-correction. Laser Raman analyses have determined the presence of CH_4 and other short-chain hydrocarbons in aqueous inclusions (Fig. **9**). Hanor's results [33] indicated that the methane content is fixed at 0.2

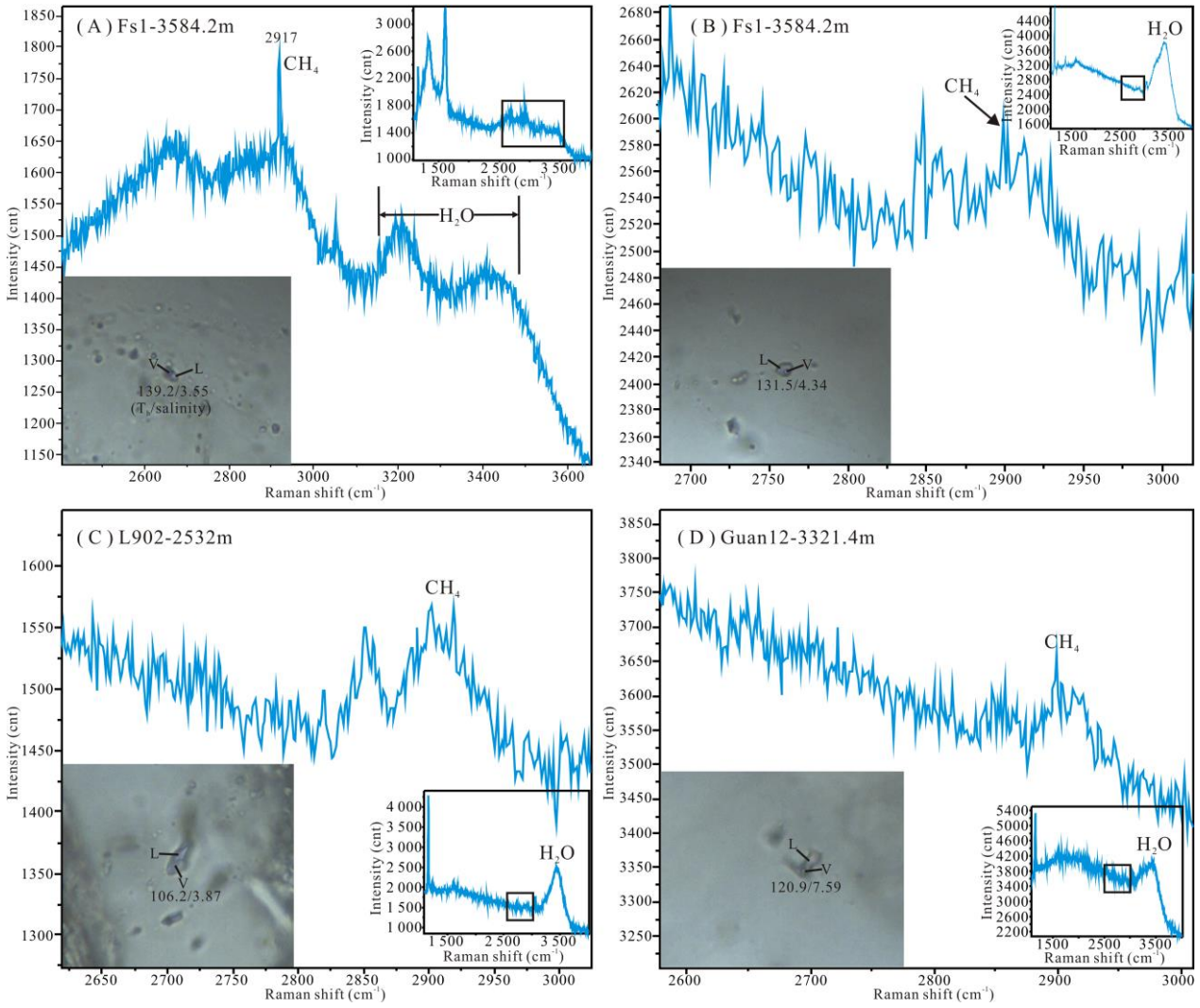

Figure 9: Characteristics of Laser Raman Spectroscopy of type Ib inclusions. The high-intensity peaks and small peak areas show the presence of a small amount of CH_4 and other short-chain hydrocarbons in aqueous inclusions.

Table 2: Homogenization temperatures of type IIb inclusions in different samples in red-bed sandstones.

Well	Depth (m)	No.	Fluorescence Under UV	Range of T_h (°C)	Average T_h (°C)	T_h of Synchronous Type Ib Inclusions (°C)
L902	2532	1	yellow	88.7	——	104.2-107.9
		3	Blue and blue white	98.2-105.3	102	121.8-124.9
Guan113	2494.49	1	yellow	87.9	——	107.5
		4	blue	99.1-107.1	102.3	118.2-127.3
Wx99	2093.08	3	blue	80.5-85.2	82.5	98.3-104.9

moles CH_4 per kg H_2O which corresponds to 3200 ppm CH_4 and is an estimated value for subsurface waters in sedimentary basins. During heating, due to the partial pressure of methane, the pressure of the bubble point line in P-T phase diagram of methane bearing aqueous inclusions is obviously higher than that of pure aqueous inclusions [33,34]. On the basis of experimental data and T_h values of inclusions from the Dongying Depression, the pressure-correction value of methane bearing inclusions is usually less than 15°C [20]. Here the T_h could be as the trapping temperatures of type Ib inclusions after being added 8-15°C, based on the empirical formula between

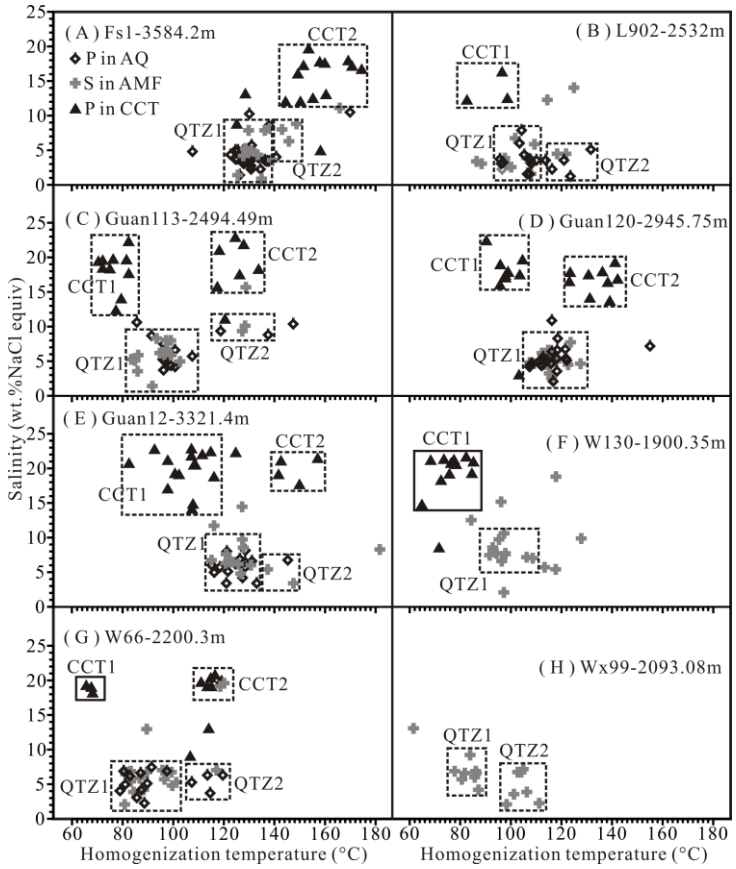

Figure 10: Salinity vs. Homogenization temperature plots for the studied fluid inclusions in authigenic quartz, AMF and carbonate cements in eight samples of red-bed reservoirs.

pressure-correction values and T_h from [20]. The true trapping pressures of type Ib inclusions were calculated as outlined in [35]. Trapping temperatures and pressures of some type Ib inclusions are listed in Table **3**. The trapping temperatures of type IIb inclusions are similar to that of synchronous type Ib inclusions.

Table 3: Trapping temperatures and pressures of some type Ib inclusions in different samples.

Well	Depth (m)	Host Minerals	Genetic Types	Salinity (eq. wt.% NaCl)	T_h (°C)	T_t (°C)	P_t (MPa)
Fs1	3584.2	AQ	P	2.74	130.8	145.8	27
Fs1	3584.2	CCT	P	16.05	149.3	164.3	32.5
Guan113	2494.49	AQ	P	6.59	100.7	109.7	17.1
Guan113	2494.49	CCT	P	22.31	82.3	87.3	12.6
Guan120	2945.75	AQ	P	8.28	118.5	130.5	22.4
Guan120	2945.75	CCT	P	17.43	97.8	105.8	19.2
L902	2532	AQ	P	4.34	105.3	115.3	18.6
L902	2532	AMF	S	4.49	121.8	133.8	22
W130	1900.35	AMF	S	7.59	97.8	104.8	13.6

Abbreviations: T_t-trapping temperature; P_t-trapping pressure; others as in Fig. (**5**) and Table **1**.

5.2. Stages of Diagenetic Fluids

The microthermometric results indicate that the red-bed reservoirs were subjected to multiple fluid events. Generally, fluid inclusions trapped at the same stage in the diagenetic process have similar T_h and salinities [16].

The Salinity vs. Homogenization temperature plots indicate that type Ib inclusions in authigenic quartz and AMF are classified into two groups (QTZ1 and QTZ2) (Fig. **10**). The T_h of the QTZ1 group is lower than that of QTZ2 group, and little difference in salinity is recorded between the two groups. The plots also indicate that the type Ib inclusions in carbonate cements define two groups (CCT1 and CCT2). The T_h of the CCT1 is lower than that of the QTZ1, while the T_h of the CCT2 is similar to or higher than that of the QTZ2. The salinities of the two groups of inclusions are similar but obviously higher than that of inclusions in authigenic quartz and AMF (Fig. **10**). Hence, type Ib inclusions in authigenic quartz, AMF and carbonate cements recorded four stages of diagenetic fluids. The type IIb inclusions are classified into two groups on the basis of fluorescence and T_h, which have the same trapping temperatures with the QTZ1 and QTZ2 respectively.

On the basis of the calculated true trapping temperatures of inclusions, the trapping times of inclusions and movement of formation fluids are obtained by putting the trapping temperatures on the corresponding burial history curves. The red-bed strata experienced the burial process of subsidence-uplift-subsidence because of the tectonic activity at the end of Dongying formation, which caused that one temperature may correspond to multiple geological times.

Fluid inclusions in authigenic quartz and AMF reflect an acid diagenetic environment while carbonate cements reflect an alkaline diagenetic environment [16]. Inclusions of group CCT1 are mainly hosted in calcites with basil style or in the middle part of pores, while inclusions of group CCT2 are mainly hosted in ferro-calcites and ankerites at the edge of pores surrounding calcites. Calcites were replaced by ferro-calcites and ankerites obviously in red-bed reservoirs [20], which indicates that the formation time of the former was earlier than that of the latter [36] and so was the primary type Ib inclusions in them. The modern formation water is a weak acid with pH ranging between 5 and 7, which provides the evidence to determine the first geological time range as the time of formation fluids recorded by inclusions of group CCT2. The movement of formation fluids recorded by inclusions of group CCT1 was the first geological time range. There was no authigenic quartz in samples with basil style calcites, the early formed calcites inhibited the development of authigenic quartz, but there was no metasomatism between calcite and authigenic quartz. The authigenic quartzes were only replaced by late formed ferro-calcites and ankerites obviously, and the phenomenon of two stages of authigenic quartz only developed in samples with low content of carbonate cements and high content of pores [20]. So, the trapping time of inclusions of group QTZ1 was later than that of group CCT1 but was earlier than that of group CCT2, and the trapping time of inclusions of group QTZ2 was later than that of group CCT2. It is impossible for inclusions reflecting different diagenetic environments trapped in the same geological time in one set of strata, which also indicates that the trapping time of inclusions of group QTZ2 was later than that of inclusions of group CCT2.

Hence, the trapping order of the four groups of type Ib inclusions in red-bed reservoirs from early to late is group CCT1, group QTZ1, group CCT2 and group QTZ2. The trapping times of the two groups of type IIb inclusions were about 28.7-27.8Ma and after 10Ma respectively. The formation order of these inclusions reflects the alternate evolution of multiple alkalines and acid formation fluids and two stages of oil filling in the diagenetic process of red-bed reservoirs.

5.3. Characteristics and Evolution of Diagenetic Fluids

The first-stage diagenetic fluid was recorded by type Ib inclusions in calcite, and the salinity was mainly between 17 and 23 eq.wt%NaCl (Fig. **11A**). Formation fluids of the early diagenetic stage were mainly influenced by syn-depositional water between sediment particles [10,11]. At the deposition period of red beds of the Dongying depression, the climate was arid, the aquatic environment was relatively closed, and clastic deposits and gypsum-salt deposits were synchronous. Therefore, syn-depositional water was characterized by high salinity and alkaline [22]. The high paleogeothermal gradient, pH and salinity and massive metallic ions in syn-depositional water promoted the transformation of clay minerals in mudstones [7]. Distribution of clay minerals indicates that the Kaolinite and smectite in interbedded mudstones of *Ek1-Es4x* transformed to illite and chlorite rapidly with high transformation degree at the early diagenetic stage [20], releasing considerable interlayer water with rich Ca^{2+}, Na^{+}, Fe^{2+}, Mg^{2+} and Si^{4+} to increase the salinity of diagenetic fluid [37]. The first-stage diagenetic fluids caused considerable and strong early calcite and gypsum cementation in red-bed reservoirs [20], which indicated that the

fluids were carbonate type and sulfate type. Compared with the relation of pH to salinity and hydrochemical type of lakes on the Qinghai-Tibet Plateau ([38], Fig. **12**), the pH of the first-stage diagenetic fluids was > 8.7 (Fig. **13**). The movement of this stage of diagenetic fluids was before 31.3Ma (Fig. **13**).

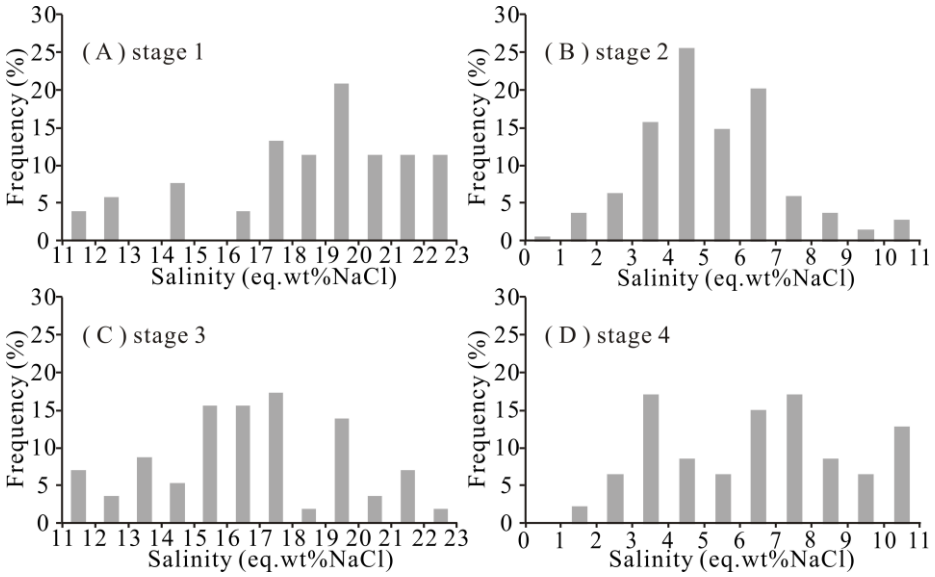

Figure 11: Salinities of the four stages of diagenetic fluids in red-bed reservoirs.

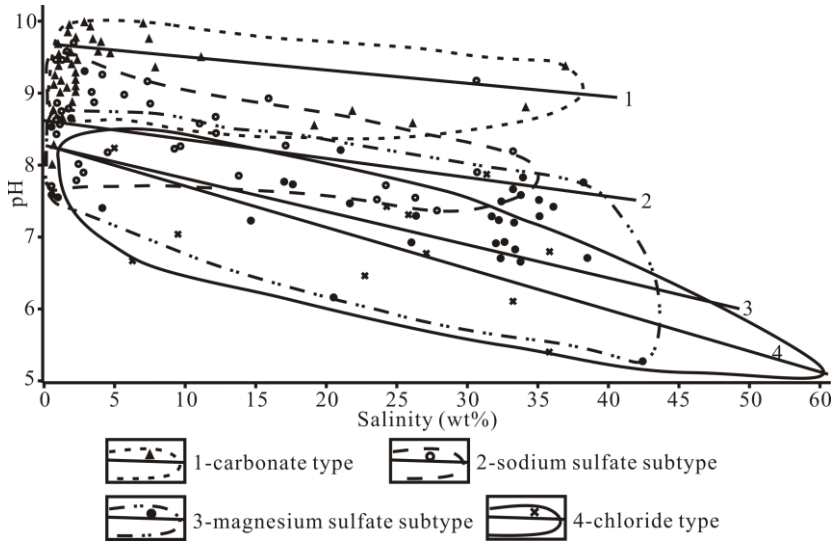

Figure 12: Relation of pH to salinity and hydrochemical type of lakes on the Qinghai-Tibet Plateau [38].

The second-stage diagenetic fluid was recorded by type Ib inclusions in authigenic quartz and AMF, and the salinity mainly ranged between 3 and 7 eq.wt%NaCl (Fig. **11B**). The diagenetic fluid was acid, and the pH mainly ranged from 5.6 to 6.1 based on the calculation of formula (1). The yellow fluorescent type IIb inclusions trapped at the same time in AMF indicated that the filling of low mature oil was accompanied [39,40]. Oil-source correlation showed that oil in red-bed reservoirs was mainly from source rocks of *Es4s* [20], which indicated that organic acids from the source rocks influenced diagenesis of red-bed reservoirs obviously. The best formation and preservation temperature of organic acid ranges from 80 to 120°C [4]. The source rocks of *Es4s* were at the immature-half mature stage within the best organic acid developing temperature range from 35.1 to 26.9Ma [22], which was consistent with the timing of 31.3-26.4Ma recorded by type Ib inclusions. During this period the source rocks released considerable organic acids and a small amount of low mature oil to neutralize the early alkaline fluids, which turned the alkaline diagenetic environment into an acidic environment (Fig. **13**).

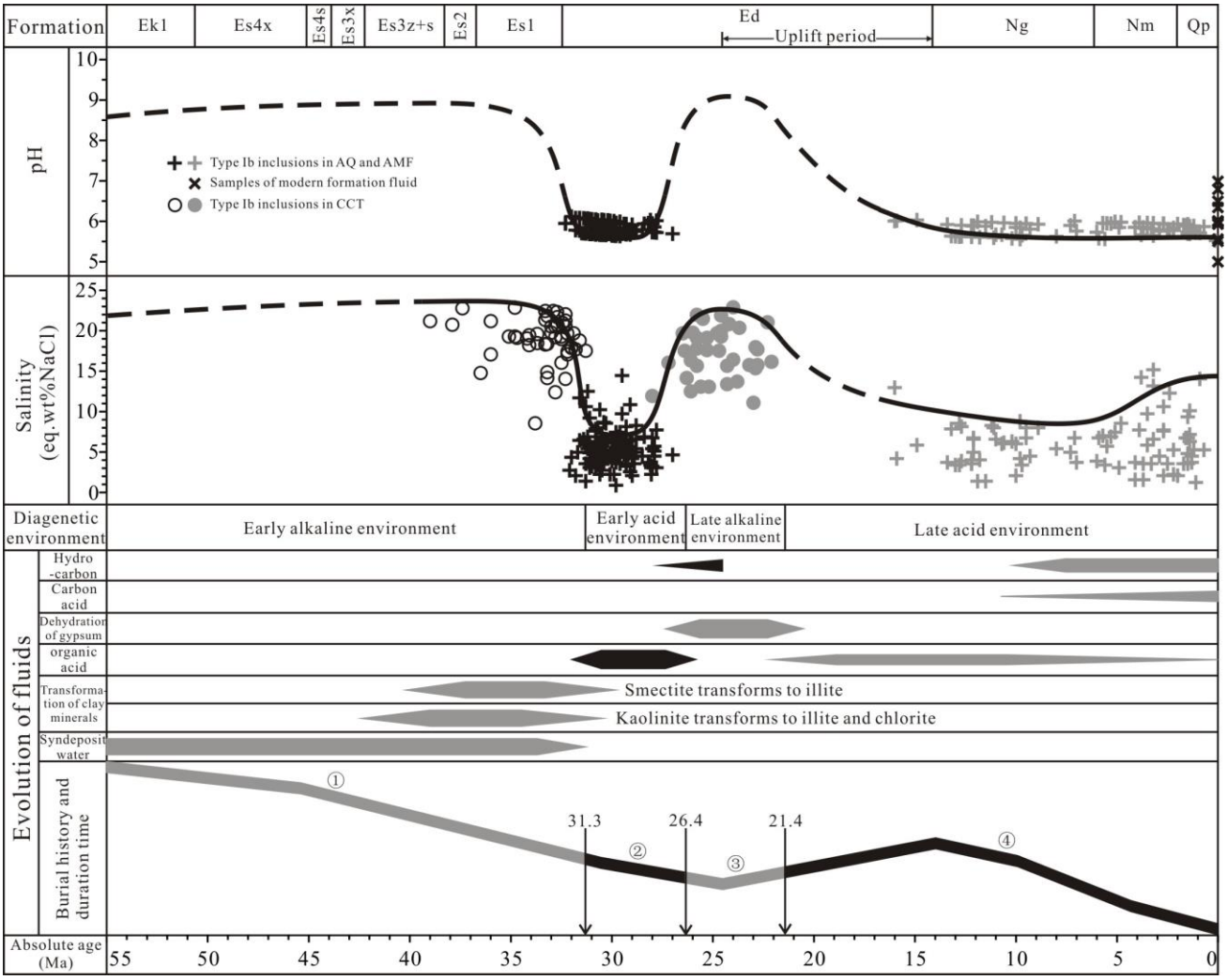

Figure 13: Evolution of diagenetic fluids in red-bed reservoirs in the Dongying depression. Abbreviations as in Fig. (**5**) and Table **1**.

The third-stage diagenetic fluid was recorded by type Ib inclusions in ferro-calcites and ankerites, and the salinity was high and mainly ranged from 15 to 20 eq.wt%NaCl (Fig. **11C**), which reflected the late alkaline fluids in red-bed reservoirs from 26.4 to 21.4Ma. The formation temperature in the sag belt reached 120-150°C during the stage of 26.9-19.8Ma [20], and the gypsum-salt rocks released considerable alkaline fluids to turn the acid diagenetic environment into an alkaline diagenetic environment. This stage of diagenetic fluids caused the late ferro-calcites and ankerites cementation in red-bed reservoirs [20], which meant that the fluids were mainly carbonate type. Compared with the relationship of pH to salinity and the hydrochemical type of lakes on the Qinghai-Tibet Plateau ([38], Fig. **12**), the pH of the third-stage diagenetic fluid was > 9 (Fig. **13**). Research results showed that the low mature hydrocarbon expulsion period continued to 24.6Ma [41], the filling of small amounts of low mature oil may be accompanied by this stage of fluid (Fig. **13**).

The fourth-stage diagenetic fluid was recorded by type Ib inclusions in authigenic quartz and AMF, and the salinity was relatively low and mainly ranged between 3 and 11 eq.wt%NaCl (Fig. **12D**). The diagenetic fluid was acid, and the pH ranged from 5.5 to 6.0 based on the calculation of formula (1). After 21.4Ma, the source rocks of *Es4s* re-entered in the temperature range suitable for the generation of organic acid [20], which turned the formation fluids from alkaline to acid. After 10Ma, source rocks of *Es4s* began to generate mature oil [41], and analysis of blue fluorescent type IIb inclusions indicated that this period was the main oil filling stage of red-bed reservoirs (Fig. **13**). With the increase of temperature, the content of organic acids in formation fluids decreased and the partial pressure of CO_2 increased gradually, which controlled the late weak acid environment ([4,42]; Fig. **13**).

Hence, during the burial history, the red-bed reservoirs experienced an evolution process of early alkaline diagenetic fluids, early acid diagenetic fluids, late alkaline diagenetic fluids and late acid diagenetic fluids, which caused the alternate evolution of multiple alkalines and acid diagenetic environments in red-bed reservoirs (Fig. **13**). The red-bed reservoirs experienced two stages of filling of oil and were dominated by the second stage of mature oil after 10Ma (Fig. **13**).

6. Conclusions

Fluid inclusions occur in authigenic quartz, carbonate cement and AMF. Inclusions in the first two kinds of minerals are primary, while in the latter type they are secondary. Both hydrocarbon and aqueous inclusions are present, the former is mainly liquid-rich two-phase and develop a range of fluorescent colors under UV, the latter could be classified into monophase, two-phase and multiphase solid inclusions based on phases observed at room temperature but are dominated by the two-phase types.

The liquid-rich two-phase aqueous inclusions were classified into four groups based on the salinity-homogenization temperature plots. The liquid-rich two-phase hydrocarbon inclusions were classified into two groups. The movement of the first-stage diagenetic fluid was before 31.3Ma, recorded by inclusions in calcites with the salinity being 17-23 eq.wt%NaCl and pH being > 8.7. Fluids were from syn-depositional water and diagenetic fluids of clay minerals in interbedded mudstones. The timing of the second-stage diagenetic fluid was between 31.3 and 26.4Ma, recorded by inclusions in authigenic quartz and AMF with the salinity being 3-7 eq.wt%NaCl and pH being 5.6-6.1. Fluids were rich in organic acids and were accompanied by the filling of small amounts of low mature oil. The timing of the third-stage diagenetic fluid was between 26.4 and 21.4Ma, recorded by inclusions in ferro-calcites and ankerites with the salinity being 15-20 eq.wt%NaCl and pH being > 9. Fluids were mainly influenced by dehydration of gypsum-salt rocks and decarboxylation of organic acids. The timing of the fourth-stage diagenetic fluid was after 21.4 Ma, recorded by inclusions in authigenic quartz and AMF with the salinity being 3-11 eq.wt%NaCl and pH being 5.5-6.0. Fluids were influenced by organic acids and carbonic acids and were accompanied by filling of considerable mature oil after 10Ma. During the burial history, the red-bed reservoirs experienced the evolution process of early alkaline diagenetic fluids, early acid diagenetic fluids, late alkaline diagenetic fluids and late acid diagenetic fluids, which caused the alternate evolution of multiple alkaline and acid diagenetic environments.

Acknowledgment

This work was co-funded by the National Key Research and Development Program of China (Grant No. 2019YFC0605501), the Shandong Provincial Natural Science Foundation (ZR2019MD004), and the Fundamental Research Funds for the Central Universities and the Development Fund of Key Laboratory of Deep Oil & Gas (20CX02102A).

References

[1] Lynch FE. Mineral/water interaction, fluid flow and sandstone diagenesis: evidence from the rocks. AAPG Bulletin 1996; 80(4): 486-504. https://doi.org/10.1306/64ED8822-1724-11D7-8645000102C1865D

[2] Alaa M, Salem S, Morad S. Diagenesis and reservoir quality evolution of fluvial sandstones during progressive burial a duplih: Evidence from the Upper Jurassic Boipeba Member, Revoncavo Basin, Northern Brazil. AAPG Bulletin 2000; 84(7): 1015-1040. https://doi.org/10.1306/A9673B9E-1738-11D7-8645000102C1865D

[3] Kharaka YK, Cole DR, Hovorka SD, Gunter WD, Knauss KG, Freifeld BM. Gas-water-rock interactions in Frio Formation following CO2 injection: Implications for the storage of greenhouse gases in sedimentary basins. Geology 2006; 34(7): 577-580. https://doi.org/10.1130/G22357.1

[4] Surdam RC, Crossey LJ, Hagen ES. Organic-inorganic and sandstone diagenesis. AAPG Bulletin 1989; 73(1): 1-23. https://doi.org/10.1306/703C9AD7-1707-11D7-8645000102C1865D

[5] Worden RH, Oxtoby NH, Smalley PC. Can oil emplacement prevent quartz cementation in sandstones? Petrol Geosci. 1998; 4(2): 129-137. https://doi.org/10.1144/petgeo.4.2.129

[6] Boles JR, Franks SG. Clay diagenesis in Wilcox sandstone of Southwest Texas: Implications of smectite diagenesis on sandstone cementation. J Sediment Petrol. 1979; 49(1): 55-70. https://doi.org/10.1306/212F76BC-2B24-11D7-8648000102C1865D

[7] Bristow TF, Milliken RE. Terrestrial perspective on authigenic clay mineral production in ancient Martian lakes. Clays Clay Minerals, 2011; 59(4): 339-358. https://doi.org/10.1346/CCMN.2011.0590401

[8] Jowett EC, Cathles LM, Davis BW. Forecast of depth of releasing water of gypsum in vaporing salt basin. Foreign Oil Gas Explorat. 1994; 6(4): 391-401.

[9] Ramm M. Porosity-depth trends in reservoir sandstones theoretical models related to Jurassic sandstones offshore Norway. Marine Petrol Geol. 1992; 9(5): 553-567. https://doi.org/10.1016/0264-8172(92)90066-N

[10] Santschi P, Höhener P, Benoit G, Brink MB. Chemical processes at the sediment-water interface. Marine Chem. 1990; 30(special issue for 32nd IU-PAC Congress): 269-315. https://doi.org/10.1016/0304-4203(90)90076-O

[11] Shaw TJ, Gieskes JM, Jahnke RA, Early diagenesis in differing depositional environments: The response of transition metals in pore water. Geochimica et Cosmochimica Acta 1990; 54(5): 1233-1246. https://doi.org/10.1016/0016-7037(90)90149-F

[12] Andrea CK, Maria M. Missing aragonitic biota and the diagenetic evolution of heterozoan carbonates: a case study from the Oligo-Miocene of the central Mediterranean. J Sediment Res. 2006; 76(5): 871-888. https://doi.org/10.2110/jsr.2006.065

[13] Roedder E. Fluid inclusions. Rev Mineral. 1984; 12: 11-45, 251-290. https://doi.org/10.1515/9781501508271

[14] Eadington PJ, Hamilton PJ. Fluid history analysis-a new concept for prospect evaluation. Australian Petrol Explorat Assoc J. 1991; 12(3): 282-294. https://doi.org/10.1071/AJ90022

[15] Wilkinson JJ, Lonergan L, Fairs T, Herrington RJ. Fluid inclusion constraints on conditions and timing of hydrocarbon migration and quartz cementation in Brent Group reservoir sandstones, Columba Terrace, northern North Sea. Geol Soc Spec Publicat. 1998; 144: 69-89. https://doi.org/10.1144/GSL.SP.1998.144.01.06

[16] Carlos R, Robert HG, Andrea C, Rafaela M. Fluid inclusions record thermal and fluid evolution in reservoir sandstones, Khatatba Formation, Western Desert, Egypt: A case for fluid injection. AAPG Bulletin 2002; 86(10): 1773-1799. https://doi.org/10.1306/61EEDD78-173E-11D7-8645000102C1865D

[17] Feng Y, Chen HH, He S, Zhao ZK, Yan J. Fluid inclusion evidence for a coupling response between hydrocarbon charging and structural movements in Yitong Basin, northeast China. J Geochem Explorat. 2010; 106(1): 84-89. https://doi.org/10.1016/j.gexplo.2010.01.009

[18] Qiu LW, Jiang ZX, Cao YC, Qiu RH, Chen WX, Tu YF. Alkaline diagenesis and its influence on reservoir rocks in Biyang Depression. Sci China (Series D) 2002; 45(7): 643-653. https://doi.org/10.1360/02yd9065

[19] Robert HG, Carlos R. Recrystallization in quartz overgrowths. J Sediment Res. 2002; 72(3): 432-440. https://doi.org/10.1306/110201720432

[20] Wang J, Cao Y, Liu K, Costanzo A, Feely M. Diagenesis and evolution of the lower eocene red-bed sandstone reservoirs in the Dongying depression, china. Marine Petrol Geol. 2018. 94: 230-245. https://doi.org/10.1016/j.marpetgeo.2018.04.011

[21] Wang J, Cao Y, Liu K, Liu J, Xue X, Xu Q. Pore fluid evolution, distribution and water-rock interactions of carbonate cements in red-bed sandstone reservoirs in the Dongying depression, china. Marine Petrol Geol. 2016; 72: 279-294. https://doi.org/10.1016/j.marpetgeo.2016.02.018

[22] Wang J, Pang Y, Cao Y, Peng J, Liu H, Sedimentary environment constraints on the diagenetic evolution of clastic reservoirs: examples from the eocene "red-bed" and "gray-bed" in the Dongying depression, china. Marine Petrol Geol. 2021; 131(2): 105153. https://doi.org/10.1016/j.marpetgeo.2021.105153

[23] Qiu NS, Li SP, Zeng JH, Thermal history and tectonic-thermal evolution of the Jiyang depression in the Bohai Bay Basin, East China. Acta Geol Sinica 2004; 78(2): 263-269 (in Chinese with English abstract).

[24] MacDonald AJ, Spooner ETC. Calibration of a Linkam TH 600 programmable heating-cooling stage for microthermometric examination of fluid inclusions. Econ Geol. 1981; 76(5): 1248-1258. https://doi.org/10.2113/gsecongeo.76.5.1248

[25] Liu B. Calculation of pH and Eh for aqueous inclusions as simple system. Acta Petrol Sinica 2011; 27(5): 1533-1542 (in Chinese with English abstract).

[26] Ryzhenko BN. Thermodynamics of equilibrium in hydrothermal solutions. Nauka, Moscow, 1981; 127.

[27] Ryzhenko BN, Bryzgalin OV. Reference neutrality points for the redox and acid-base properties of aqueous solutions at the parameters for hydrothermal ore formation. Geokhimiya 1984; 7: 1056-1064.

[28] Lu HZ, Fan HR, Ni P, Ou GX, Shen K, Zhang WH. Fluid inclusions. Beijing: Science Publishing House, 2004; 370-371 (in Chinese).

[29] Murry AC, Roedder E. Fluid inclusions evidence on the environments of sedimentary diagenesis, a review. SEPM Spec Publicat. 1979; 26: 157-203. https://doi.org/10.2110/pec.79.26.0089

[30] Oakes CS, Bodnar RJ, Simonson JM. The system NaCl-CaCl2-H2O: I. The ice liquidus at 1 atm total pressure. Geochim Cosmochim Acta 1990; 54(3): 603-610. https://doi.org/10.1016/0016-7037(90)90356-P

[31] Oakes CS, Simonson JM, Bodnar RJ. The system NaCl-CaCl2-H2O: II. Densities for ionic strengths of 0.1-19.2 mol·kg-1 at 298.15-308.15K and at 0.1Mpa. J Chem Eng Data 1990; 35: 304-309. https://doi.org/10.1021/je00061a022

[32] Dubessy J, Poty B, Ramboz C. Advances in C O H N S fluid geochemistry based on micro-Raman spectrometric analysis of fluid inclusions. Eur J Mineral. 1989; 1(4): 517-534. https://doi.org/10.1127/ejm/1/4/0517

[33] Hanor JS. Dissolved methane in sedimentary brines: potential effect on the PVT properties of fluid inclusions. Econ Geol. 1980; 75: 603-617. https://doi.org/10.2113/gsecongeo.75.4.603

[34] Goldstein RH, Reynolds TJ. Systematics of fluid inclusions and diagenetic minerals. SEPM Short course, Printed in USA 1994; 31: 1-199. https://doi.org/10.2110/scn.94.31.0001

[35] Zhang YG, Frantz JD. Determination of the homogenization temperatures and densities of supercritical fluids in the system NaCl-KCl-CaCl2-H2O using synthetic fluid inclusions. Chem Geol. 1987; 64(3-4): 335-350. https://doi.org/10.1016/0009-2541(87)90012-X

[36] Tobin RC, McClain T, Lieber RB, Ozkan A, Banfield LA, Marchand AME, McRae LE. Reservoir quality modeling of tight-gas sands in Wamsutter field: Integration of diagenesis, petroleum systems, and production data. AAPG Bulletin 2010; 94(8): 1229-1266. https://doi.org/10.1306/04211009140

[37] Merriman RJ. Clay minerals and sedimentary basin history. Eur J Mineral. 2005; 17(1): 7-20. https://doi.org/10.1127/0935-1221/2005/0017-0007

[38] Zheng MP, Liu XF. Hydrochemistry of salt lakes of the Qinghai-Tibet Plateau, China Saline lakes and global change. Aquat Geochem. 2009; 15(11): 293-320. https://doi.org/10.1007/s10498-008-9055-y

[39] Stasiuk LD, Snowdon LR. Fluorescence micro-spectrometry of synthetic and natural hydrocarbon fluid inclusion: Crude oil chemistry, density and application to petroleum migration. Appl Geochem. 1997; 12(3): 229-241. https://doi.org/10.1016/S0883-2927(96)00047-9

[40] Munz IA. Petroleum inclusions in sedimentary basins: Systematics, analytical methods and applications. Lithos 2001; 55(1-4): 195-212. https://doi.org/10.1016/S0024-4937(00)00045-1

[41] Guo XW, He S, Liu KY, Song GQ, Wang XJ, Shi ZS. Oil generation as the dominant overpressure mechanism in the Cenozoic Dongying depression, Bohai Bay Basin, China. AAPG Bulletin 2010; 94(12): 1859-1881. https://doi.org/10.1306/05191009179

[42] Tissot BP, Welte DH, Petroleum formation and occurrence: Springer-Verlag, Berlin, 1984; pp. 699. https://doi.org/10.1007/978-3-642-87813-8